Surface Improvement of Halloysite Nanotubes

Tayser Sumer Gaaz [1,2,*], Abu Bakar Sulong [1,*], Abdul Amir H. Kadhum [3], Mohamed H. Nassir [4] and Ahmed A. Al-Amiery [5]

[1] Department of Mechanical & Materials Engineering, Faculty of Engineering & Built Environment, University Kebangsaan Malaysia, Bangi 43600, Selangor, Malaysia

[2] Department of Machinery Equipment Engineering Techniques, Technical College Al-Musaib, Al-Furat Al-Awsat Technical University, Al-Musaib, Babil 51009, Iraq

[3] Department of Chemical & Process Engineering, Faculty of Engineering & Built Environment, Universiti Kebangsaan Malaysia, Bangi 43600, Selangor, Malaysia; amir@eng.ukm.my

[4] Program of Chemical Engineering, Taylor's University-Lakeside Campus, Subang Jaya 47500, Selangor, Malaysia; mohamedh.nassir@taylors.edu.my

[5] Environmental Research Center, University of Technology (UOT), Baghdad 10001, Iraq; dr.ahmed1975@gmail.com

* Correspondence: taysersumer@gmail.com (T.S.G.); abubakar@ukm.edu.my (A.B.S.); Tel.: +60-11-210-60892 (T.S.G.); +60-38-921-6678 (A.B.S.); Fax: +60-38-925-9659 (A.B.S.)

Abstract: A novel development on halloysite-polyvinyl alcohol (HNTs-PVA) nanocomposites has been conducted using malonic acid (MA) by crosslinking PVA and HNTs. PVA-MA crosslinking produces smooth surfaces, which play an important role in enhancing the properties of HNTs-PVA nanocomposite. The crystallographic structures of crosslinked HNTs-PVA show almost no change as depicted by the X-ray diffraction (XRD)-2θ-peak, suggesting that MA has no or little influence on the crystallographic structure of the HNTs-PVA. Images taken by field emission scanning electron microscope (FESEM) suggest possible effects of MA on the morphology and internal features of HNTs-PVA by reducing the agglomeration of HNTs, which is considered a decisive step in improving the surface qualities of HNTs. Investigating the samples using the Brunauer–Emmelt–Teller (BET) technique showed that the surface area was increased by about 10 times, reaching the second highest recorded results compared to the HNTs, which could be considered a breakthrough step in enhancing the properties of HNTs-PVA due to MA crosslinking.

Keywords: halloysite; nanotubes; polyvinyl; malonic acid

1. Introduction

Malonic acid (MA) plays an important role as a competitive inhibitor [1] and as a crosslinker with minimal toxicity compared to glutaraldehyde or glyoxal [2]. MA produces numerous valuable and biodegradable compounds [3] that are commonly used in foam packaging, bags, and other related products. The mechanism of using MA as a crosslinker was described by Qiu and Netravali [4]. When individualized hydrophobic halloysite nanotubes (HNTs) [5] are mixed with polyvinyl alcohol (PVA), HNTs-PVA is characterized as a fully biodegradable nanocomposite [4] with enhanced mechanical properties. Nanotubes such as HNTs [6–9] or carbon nanotubes (CNTs) [10] are very effective with even small quantities of loading with polymers such as thermoplastic nanoparticles, which could result in significant changes in the physical and chemical properties. The thermoplastic polymers, such as PVA, are also biocompatible polymers that are widely used in industry for films, paper, and adhesive coating due to their attractive properties [11,12]. Crosslinking has been utilized to improve the thermo-physical properties including the solubility of many polymers [13,14].

Throughout the process of sample preparation, sodium dodecyl sulfate (SDS) is used as a good dispersing agent for HNTs in aqueous solution [15,16]. The chemical structure of HNTs shows that the external surface contains siloxane (Si–O–Si) groups, aluminol (Al–OH), and silanol (Si–OH) groups [17,18]. The effect of the biopolymer charge on nanocomposite materials was thoroughly discussed in [19]. HNTs possess a much better dispersion property and potential ability for the formation of hydrogen bonding [20] than other natural silicates such as montmorillonite and kaolinite. HNTs were acid-treated by Abdullayev et al. [21,22] and Zhang et al. [23] who reported improvement in the specific surface area to 250 m^2/g and 267 m^2/g from about 60 m^2/g, respectively. HNTs' wear resistance was discussed by [24] while creating a mechanically robust spray of epoxy-coated halloysite composites was discussed in [25]. Recently, two publications, Shu et al. [26] and Gaaz et al. [27], both in press, have shown that the specific surface area was improved to new frontiers, as far as 608 m^2/g and 306 m^2/g, by treating HNTs with alkali solution, followed by acid etching, respectively. Briefly, esterification is obtained via PVA-MA crosslinking [28,29]. Researchers have been exploring different levels for the effectiveness of MA crosslinking while their expectations varied within a reasonable level of differences, especially in thermal properties. The highest level of HNTs-PVA nanocomposite was achieved by producing water-insoluble PVA [30]. The qualities of the composite by individualization of HNTs with the assistance of MA crosslinking with PVA were also studied [31]. In this work, the specific surface area was improved to 511 m^2/g from about 60 m^2/g for neat HNTs, which is considered the second highest increase to the best of our knowledge.

2. Results and Discussion

2.1. X-ray Diffraction (XRD)

XRD patterns of different samples exhibited characteristic reflections of the four samples S0, S05, S07, and S10, as shown in Figure 1. A view of a single HNT crystal with clear representation of the crystal axes is included as the insert in Figure 1 [32]. Reflections of S0 were detected at *2θ* = 11.2°, 20.1°, 25.2°, 26.9°, 27.6°, 35.9°, 50.1°, 55.4°, 60.1°, 62.9°, 68.2°. Apparently, XRD peaks of the modified HNTs nearly remained consistent with the neat HNTs. After surface modification, there was no indication of significant change in the XRD peaks, implying that the crystal structure of HNTs was not altered [33].
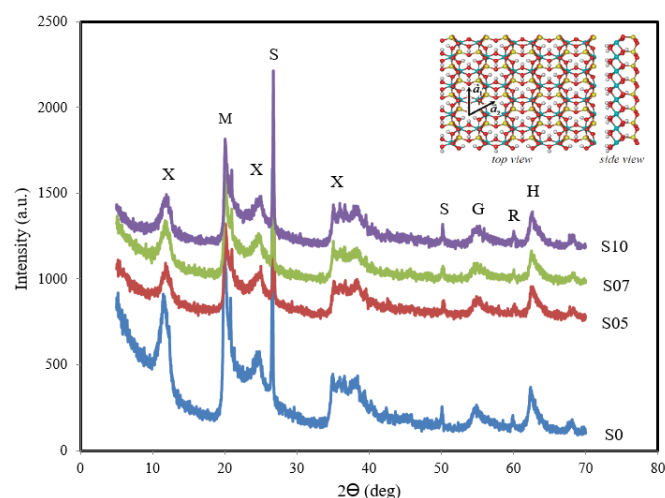

Figure 1. XRD patterns of S0, S05, S07, and S10. X, halloysite (7 Å); M, sodium aluminum silicon oxide; S, quartz; R, silicon oxide; G, graphite.

2.2. Field Emission Scanning Electron Microscope (FESEM)

Figure 2 shows the FESEM images of S0, S05, S07, and S10. Based on the capability of FESEM, the images of the samples show the bulk of the sample rather than the surface. Sample S0 shows

several sizes of HNTs, shown in Figure 2a. By adding SDS, PVA and MA at 5 wt. % to the mixture of HNTs and distilled water, the effects of these treatments are shown in the subsequent FESEM images. Apparently, HNTs were significantly affected by the treatment, as many HNTs were broken, as shown in Figure 2b. The condition of S07, shown in Figure 2c, was improved as the treatment increased from 5 wt. % to 7 wt. % of SDS, PVA, and MA. S07 underwent some changes, which resulted in improving the condition of the bulk sample by showing that the number of intact HNTs was higher than S05 and the distribution was better. As the mixture of HNTs and distilled water was treated with 10 wt. % of SDS, PVA, and MA, as shown in Figure 2d, the crosslinking caused by MA showed better distribution and the number of intact HNTs was increased. The agglomeration of HNTs in the nanocomposite significantly decreased.
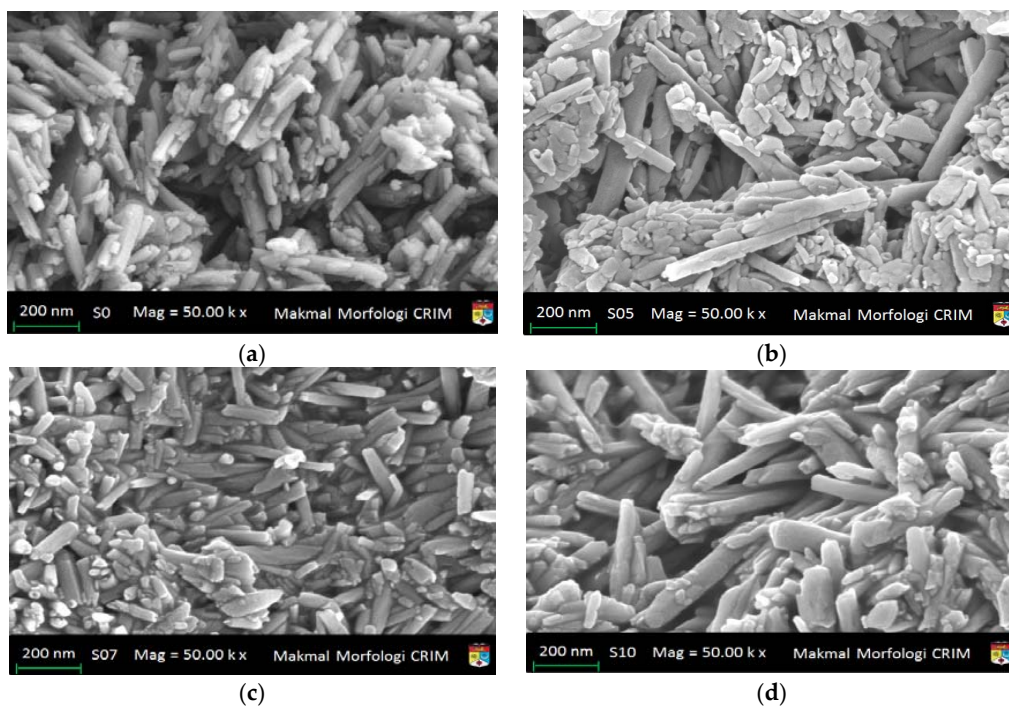

Figure 2. FESEM microphotographs for: (**a**) S0; (**b**) S05; (**c**) S07; and (**d**) S10.

2.3. Brunauer–Emmelt–Teller (BET)

N_2 adsorption-desorption isotherms of S0, S05, S07, and S10 with the distinct-type H_3 hysteresis loop are shown in Figure 3a, while the distribution of the microspore sizes of the same set is shown in Figure 3b. The BET results are listed in Table 1. The parameters under consideration included the BET surface area and total pore volume. For the S0 sample, the BET surface area and the total pore volume were recorded at 59.04 m^2/gm and 0.26 cm^3/g, respectively. The results of S0 are in agreement with other findings [26]. As the treatment of HNTs is conducted by adding SDS, PVA, and MA at 5%, 7%, and 10%, the BET surface area decreased to 40.13 m^2/gm (about a 30% decrease) for S05, and then moderately increased to 54.68 m^2/gm, almost approaching the level of S0. The result of 30% less surface area goes very well with the reduction of the total pore volume from 0.26 to 0.23 cm^3/gm (density increases from 3.84 to 4.34 gm/cm^3). As the treatment increased to 7% (sample S07), the BET surface area increased while the average pore size decreased, suggesting that S07 became less porous due to the crosslinking process. When the treatment was increased to 10%, BET was significantly increased to 511.12 m^2/gm. This increase goes very well with the results of the total pore volume which decreased by almost the same percentage as the BET surface area. The results of the average pore size of S10 do not reflect these significant changes; however, the number of pores (not the size)

could support the results by assuming that the surface and the bulk of S10 have a huge increase in the number of the pores, which makes S10 very porous compared to the S0 sample, as shown in Figure 3b.

Table 1. Surface areas and pore volumes of neat HNTs and HNTs crosslinked with MA.

Sample	S0	S05	S07	S10
BET surface area (m^2/gm)	59.04	40.13	54.68	511.12
Total pore volume (cm^3/gm)	0.26	0.23	0.25	2.35

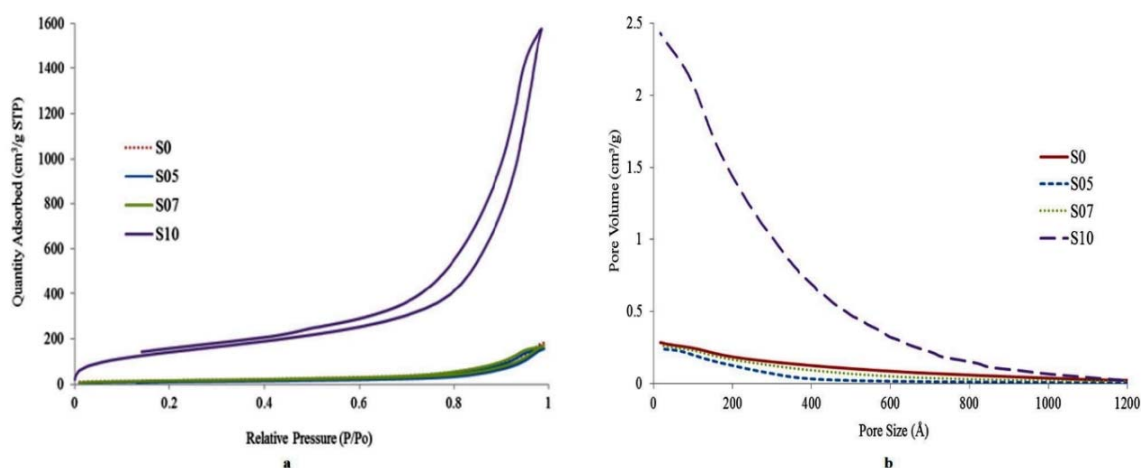**Figure 3.** (**a**) N_2 adsorption-desorption curves; (**b**) Distribution micropore size.

3. Experimental Section

3.1. Materials

Natural Nano, Inc., 832 Emerson Street Rochester, New York, NY, USA, supplied HNTs. Tables 2 and 3 contain the chemical compositions and physical properties of HNTs, respectively. Other chemicals used in this work and their properties are presented in Table 4.

Table 2. Chemical composition of HNTs.

Chemical Compositions	SiO_2	Al_2O_3	TiO_2	Fe_2O_3	MgO
Weight %	61.19	18.11	20.11	0.49	0.10

Table 3. Physical properties of HNTs.

Chemical Formula	Surface Area	Pore Volume	Density	Refractive Index
$Al_2Si_2O_5(OH)_4 \cdot nH_2O$	60 m^2/g	~1.25 mL/g	2540 kg/m^3	1.54

Table 4. Other chemicals used in this work and their properties.

Materials	Typical Data	Unit	Value	Sources
SDS ($C_{12}H_{25}NaO_4S$)	Molecular Weight	g/mol	288.38	BioShop Canada Inc., Burlington, ON, Canada
	Melting Point	°C	204–207	
	pH	-	9.5	
	Specific Gravity	-	1.11	
PVA	Molecular Weight	g/mol	89–98	Sigma Aldrich, St. Louis, MI, USA
	pH	-	5–7	
	Viscosity	cps	11.6–15.4	
	Density	g/cm^3	1.27	
MA ($C_3H_4O_4$)	Molecular Weight	g/mol	104.06	Sigma Aldrich, St. Louis, MI, USA
	Purity	%	98.5–101.5	

3.2. Procedures of HNTs-PVA Crosslinked with MA

The preparation of the samples was performed throughout four steps as shown in Table 5 and schematically in Figure 4. Firstly, a mixture of 1.0 g HNTs (powder) added to 50 g distilled water at room temperature. The mixture was then treated with 0.05 g of SDS followed by adding 0.05 g of PVA (powder) to the mixture. The final mixture was then treated with 0.05 g MA for crosslinking. For the other two samples, the wt. percentage of 0.07 g and 0.10 g were separately added instead of 0.05 g of SDS, PVA, or MA. The addition of SDS facilitates the dispersion as noted in [16,34]. The mixtures produced in step IV are stirred separately for 1 h at 90 °C at speed of 500 rpm. Then, the samples were taken for sonication at 60 °C for 10 min and are dried slowly in an oven at 40 °C. The three samples are labeled as S05, S07, and S10 based on the wt. percentage of SDS, PVA, or MA, where S refers to sample. The samples are ground separately using a grinding mortar. For completeness, the neat HNTs sample is denoted as S0.

Table 5. Samples preparation.

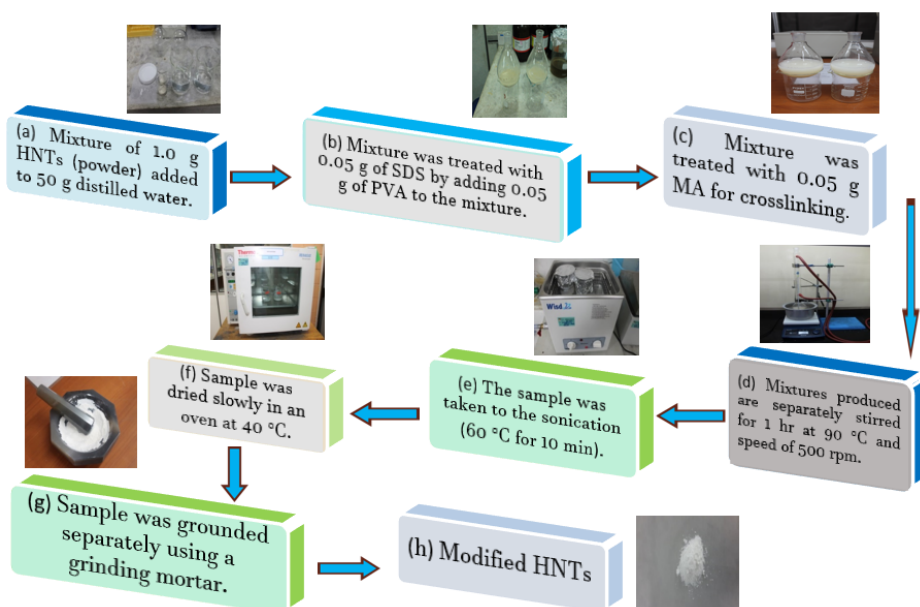| Samples	Step I	Step II	Step III	Step IV
S05	HNTs (1.0 g) + H_2O (50 g)	+SDS (0.05 g)	+PVA (0.05 g)	+MA (0.05 g)
S07	HNTs (1.0 g) + H_2O (50 g)	+SDS (0.07 g)	+PVA (0.07 g)	+MA (0.07 g)
S10	HNTs (1.0 g) + H_2O (50 g)	+SDS (0.10 g)	+PVA (0.10 g)	+MA (0.10 g)

Figure 4. Procedure of crosslinked HNTs-PVA nanocomposites using MA.

3.3. Characterization: Apparatus and Techniques

Investigating HNTs, PVA, and HNTs-PVA nanocomposites are conducted through several techniques. Firstly, the HNTs structure and crystallite size are investigated using XRD model D8 with advance Bruker AXS X-ray and Cu radiation of 1.5406 Å (Berlin, Germany). XRD is equipped with the EVA software (Version 2, Manufacturer, Karsruhe, Germany) to evaluate the structure and lattice strain of samples. All XRD patterns are compared for standardization with the Joint Committee on Powder Diffraction Standards (JCPDS). Regarding morphological images of the HNTs, field emission scanning electron microscope (FESEM) of model Zeiss SUPRA 55-VP (Manufacturer, Konigsallee, Germany) was used. This model is equipped with a higher resolution and it has a lower charging on the sample surface. The magnifications of the morphology observations are set at 50.00 kx. Finally,

Brunauer–Emmelt–Teller (BET) was used to show the physical adsorption of gas molecules to specify the effective surface area using (V-Sorb 2800TP). BET analysis including surface area, pore size, and distribution, and pore volume, was performed using a Gemini apparatus (Micrometrics ASAP 2020, Norcross, GA, USA) of accuracy of ± 0.02 m^2/g. Samples are degassed in a vacuum of 50 mTorr and at 350 °C for 2 h. The Barrett–Joyner–Halenda (BJH) equation is used to calculate the pore volume as well as the average pore size of the distribution by exploiting the nitrogen desorption isotherm [35]. The total surface area of the sample can be determined by the number of nitrogen molecules obtained from the desorption–adsorption results.

4. Conclusions

HNTs-PVA nanocomposites have been investigated by numerous numbers of researchers due to their wide applications in industry and medical fields. HNTs-PVA crosslinking is a relatively new technique. In this work, MA was added at 5 wt. %, 7 wt. %, and 10 wt. % to the mixture of HNTs-PVA, creating three samples, S05, S07, and S10, which were investigated and compared to the neat HNTs in sample S0. The samples were examined using XRD, FESEM and BET. FESEM images of S05 and S07 showed that HNTs are well distributed. FESEM images of the four samples showed a possible effect of MA on the morphology and internal features of HNTs-PVA by showing less HNT agglomeration as indicative of the effect of SDS. The XRD results showed almost no difference in the 2θ-peak, suggesting that adding MA has little effect on the crystallography of the treated samples. The BET investigation showed that the surface area was increased by about 10 times compared to the HNTs, achieving the level of 511 m^2/g. This result, the second highest recorded result, is considered a breakthrough in enhancing the properties of HNTs-PVA treated by MA crosslinking, which may be attributed to the size and number of the pores.

Author Contributions: Tayser Sumer Gaaz was a PhD student who did all experiments as part of his project. Mohamed H. Nassir helped with characterization of the nanomaterial. Abu Bakar Sulong and Abdul Amir H. Kadhum were the principal investigators, and Ahmed A. Al-Amiery was a co-investigator. All authors are aware of this manuscript and have agreed to its publication.

Conflicts of Interest: The authors declare no conflict of interest.

References

1. Belsky, A.; Maiella, P.; Brill, T. Spectroscopy of hydrothermal reactions 13. Kinetics and mechanisms of decarboxylation of acetic acid derivatives at 100–260 °C under 275 bar. *J. Phys. Chem. A* **1999**, *103*, 4253–4260. [CrossRef]

2. Qiu, K. Biobased and Biodegradable Polymer Nanocomposites. Ph.D. Thesis, Cornell University, Ithaca, NY, USA, 2012.

3. Pollak, P.; Vouillamoz, R. *Fine Chemicals*; Wiley Online Library: Hoboken, NJ, USA, 2011.

4. Qiu, K.; Netravali, A.N. Halloysite nanotube reinforced biodegradable nanocomposites using noncrosslinked and malonic acid crosslinked polyvinyl alcohol. *Polym. Compos.* **2013**, *34*, 799–809. [CrossRef]

5. Cavallaro, G.; Lazzara, G.; Milioto, S.; Parisi, F. Hydrophobically modified halloysite nanotubes as reverse micelles for water-in-oil emulsion. *Langmuir* **2015**, *31*, 7472–7478. [CrossRef] [PubMed]

6. Liu, M.; Guo, B.; Du, M.; Jia, D. Drying induced aggregation of halloysite nanotubes in polyvinyl alcohol/halloysite nanotubes solution and its effect on properties of composite film. *Appl. Phys. A* **2007**, *88*, 391–395. [CrossRef]

7. Joussein, E.; Petit, S.; Churchman, J.; Theng, B.; Righi, D.; Delvaux, B. Halloysite clay minerals—A review. *Clay Miner.* **2005**, *40*, 383–426. [CrossRef]

8. Gaaz, T.S.; Sulong, A.B.; Akhtar, M.N.; Kadhum, A.A.H.; Mohamad, A.B.; Al-Amiery, A.A. Properties and applications of polyvinyl alcohol, halloysite nanotubes and their nanocomposites. *Molecules* **2015**, *20*, 22833–22847. [CrossRef] [PubMed]

9. Cavallaro, G.; Lazzara, G.; Milioto, S.; Parisi, F.; Sparacino, V. Thermal and dynamic mechanical properties of beeswax-halloysite nanocomposites for consolidating waterlogged archaeological woods. *Polym. Degrad. Stab.* **2015**, *120*, 220–225. [CrossRef]

10. Rousakis, T.C.; Kouravelou, K.B.; Karachalios, T.K. Effects of carbon nanotube enrichment of epoxy resins on hybrid FRP–FR confinement of concrete. *Compos. B Eng.* **2014**, *57*, 210–218. [CrossRef]

11. Solaro, R.; Corti, A.; Chiellini, E. Biodegradation of poly (vinyl alcohol) with different molecular weights and degree of hydrolysis. *Polym. Adv. Technol.* **2000**, *11*, 873–878. [CrossRef]

12. Chiellini, E.; Corti, A.; D'Antone, S.; Solaro, R. Biodegradation of poly (vinyl alcohol) based materials. *Prog. Polym. Sci.* **2003**, *28*, 963–1014. [CrossRef]

13. Yeom, C.-K.; Lee, K.-H. Pervaporation separation of water-acetic acid mixtures through poly (vinyl alcohol) membranes crosslinked with glutaraldehyde. *J. Membr. Sci.* **1996**, *109*, 257–265. [CrossRef]

14. Zhang, Y.; Zhu, P.C.; Edgren, D. Crosslinking reaction of poly (vinyl alcohol) with glyoxal. *J. Polym. Res.* **2010**, *17*, 725–730. [CrossRef]

15. Lin, Y.; Ng, K.M.; Chan, C.-M.; Sun, G.; Wu, J. High-impact polystyrene/halloysite nanocomposites prepared by emulsion polymerization using sodium dodecyl sulfate as surfactant. *J. Colloid Interface Sci.* **2011**, *358*, 423–429. [CrossRef] [PubMed]

16. Cavallaro, G.; Lazzara, G.; Milioto, S. Exploiting the colloidal stability and solubilization ability of clay nanotubes/ionic surfactant hybrid nanomaterials. *J. Phys. Chem. C* **2012**, *116*, 21932–21938. [CrossRef]

17. Yuan, P.; Tan, D.; Annabi-Bergaya, F. Properties and applications of halloysite nanotubes: Recent research advances and future prospects. *Appl. Clay Sci.* **2015**, *112*, 75–93. [CrossRef]

18. Gaaz, T.; Sulong, A.; Ansari, M.; Kadhum, A.; Al-Amiery, A.; Al-Furjan, M. Effect of halloysite nanotubes loading on thermo-mechanical and morphological properties of polyurethane nanocomposites. *Mater. Technol.* **2016**, 1–13. [CrossRef]

19. Bertolino, V.; Cavallaro, G.; Lazzara, G.; Merli, M.; Milioto, S.; Parisi, F.; Sciascia, L. Effect of the biopolymer charge and the nanoclay morphology on nanocomposite materials. *Ind. Eng. Chem. Res.* **2016**, *55*, 7373–7380. [CrossRef]

20. Du, M.; Guo, B.; Lei, Y.; Liu, M.; Jia, D. Carboxylated butadiene–styrene rubber/halloysite nanotube nanocomposites: Interfacial interaction and performance. *Polymer* **2008**, *49*, 4871–4876. [CrossRef]

21. Abdullayev, E.; Joshi, A.; Wei, W.; Zhao, Y.; Lvov, Y. Enlargement of halloysite clay nanotube lumen by selective etching of aluminum oxide. *ACS Nano* **2012**, *6*, 7216–7226. [CrossRef] [PubMed]

22. Vergaro, V.; Abdullayev, E.; Lvov, Y.M.; Zeitoun, A.; Cingolani, R.; Rinaldi, R.; Leporatti, S. Cytocompatibility and uptake of halloysite clay nanotubes. *Biomacromolecules* **2010**, *11*, 820–826. [CrossRef] [PubMed]

23. Zhang, A.-B.; Pan, L.; Zhang, H.-Y.; Liu, S.-T.; Ye, Y.; Xia, M.-S.; Chen, X.-G. Effects of acid treatment on the physico-chemical and pore characteristics of halloysite. *Colloids Surf. A Physicochem. Eng. Asp.* **2012**, *396*, 182–188. [CrossRef]

24. Song, K.; Chen, D.; Polak, R.; Rubner, M.F.; Cohen, R.E.; Askar, K.A. Enhanced Wear Resistance of Transparent Epoxy Composite Coatings with Vertically Aligned Halloysite Nanotubes. *ACS Appl. Mater. Interfaces* **2016**. [CrossRef] [PubMed]

25. Song, K.; Polak, R.; Chen, D.; Rubner, M.F.; Cohen, R.E.; Askar, K.A. Spray-Coated Halloysite–Epoxy Composites: A Means To Create Mechanically Robust, Vertically Aligned Nanotube Composites. *ACS Appl. Mater. Interfaces* **2016**, *8*, 20396–20406. [CrossRef] [PubMed]

26. Shu, Z.; Chen, Y.; Zhou, J.; Li, T.; Sheng, Z.; Tao, C.; Wang, Y. Preparation of halloysite-derived mesoporous silica nanotube with enlarged specific surface area for enhanced dye adsorption. *Appl. Clay Sci.* **2016**. [CrossRef]

27. Gaaz, T.S.; Sulong, A.B.; Kadhum, A.A.H.; Nassir, M.H.; Al-Amiery, A.A. Impact of sulfuric acid treatment of halloysite on physico-chemic properties modification. *Materials* **2016**. [CrossRef]

28. Jian, S.; Ming, S.X. Crosslinked PVA-PS thin-film composite membrane for reverse osmosis. *Desalination* **1987**, *62*, 395–403. [CrossRef]

29. Majumdar, S.; Adhikari, B. Polyvinyl alcohol: A taste sensing material. *Sens. Actuators B Chem.* **2006**, *114*, 747–755. [CrossRef]

30. Zhou, W.Y.; Guo, B.; Liu, M.; Liao, R.; Rabie, A.B.M.; Jia, D. Poly(vinyl alcohol)/halloysite nanotubes bionanocomposite films: Properties and in vitro osteoblasts and fibroblasts response. *J. Biomed. Mater. Res. A* **2010**, *93*, 1574–1587. [CrossRef] [PubMed]

31. Biddeci, G.; Cavallaro, G.; di Blasi, F.; Lazzara, G.; Massaro, M.; Milioto, S.; Parisi, F.; Riela, S.; Spinelli, G. Halloysite nanotubes loaded with peppermint essential oil as filler for functional biopolymer film. *Carbohydr. Polym.* **2016**, *152*, 548–557. [CrossRef] [PubMed]

32. Guimaraes, L.; Enyashin, A.N.; Seifert, G.; Duarte, H.A. Structural, electronic, and mechanical properties of single-walled halloysite nanotube models. *J. Phys. Chem. C* **2010**, *114*, 11358–11363. [CrossRef]

33. Tang, Y.; Zhou, D.; Zhang, J. Novel polyvinyl alcohol/styrene butadiene rubber latex/carboxymethyl cellulose nanocomposites reinforced with modified halloysite nanotubes. *J. Nanomater.* **2013**. [CrossRef]

34. Cavallaro, G.; Lazzara, G.; Milioto, S.; Parisi, F.; Sanzillo, V. Modified halloysite nanotubes: Nanoarchitectures for enhancing the capture of oils from vapor and liquid phases. *ACS Appl. Mater. Interfaces* **2013**, *6*, 606–612. [CrossRef] [PubMed]

35. Rouquerol, J.; Rouquerol, F.; Llewellyn, P.; Maurin, G.; Sing, K.S. *Adsorption by Powders and Porous Solids: Principles, Methodology and Applications*; Academic Press: Cambridge, MA, USA, 2013.